



Short communication

## Enhanced catalytic properties from platinum nanodots covered carbon nanotubes for proton-exchange membrane fuel cells

Zhe Tang<sup>a</sup>, Chee Kok Poh<sup>b</sup>, Kian Keat Lee<sup>c</sup>, Zhiqun Tian<sup>b</sup>, Daniel H.C. Chua<sup>a,\*</sup>, Jianyi Lin<sup>b</sup><sup>a</sup> Department of Materials Science and Engineering, National University of Singapore, 7 Engineering Drive 1, Singapore 117574, Singapore<sup>b</sup> Institute of Chemical and Engineering Sciences, 1 Pesek Road, Jurong Island, Singapore 627833, Singapore<sup>c</sup> NUS Nanoscience & Nanotechnology Initiative (NUSNNI), 2 Science Drive 3, Singapore 117542, Singapore

## ARTICLE INFO

## Article history:

Received 19 March 2009

Received in revised form 12 June 2009

Accepted 26 June 2009

Available online 10 July 2009

## Keywords:

Proton-exchange membrane fuel cell

Carbon nanotube

Platinum

Sputtering

Power density

## ABSTRACT

An efficient fabrication method for carbon nanotube (CNT)-based electrode with a nanosized Pt catalyst is developed for high efficiency proton-exchange membrane fuel cells (PEMFC). The integrated Pt/CNT layer is prepared by in situ growth of a CNT layer on carbon paper and subsequent direct sputter-deposition of the Pt catalyst. Both scanning electron microscopy (SEM) and transmission electron microscopy (TEM) demonstrate that this Pt/CNT layer consists of a highly porous CNT layer covered by well-dispersed Pt nanodots with a narrow size distribution. Compared with conventional gas-diffusion layer assisted electrodes, the CNT-based electrode with a Pt/CNT layer acting as a combined gas-diffusion layer and catalyst layer shows pronounced improvement in polarization tests. A high maximum power density of 595 mW cm<sup>-2</sup> is observed for a low Pt loading of 0.04 mg cm<sup>-2</sup> at the cathode.

© 2009 Elsevier B.V. All rights reserved.

### 1. Introduction

Carbon nanotubes have attracted great interest in recent years because of their promising applications as catalyst-support materials in fuel cells. Currently, a number of studies have shown a growing trend in the use of carbon nanotubes (CNT) to replace carbon black (CB) as catalyst support for proton-exchange membrane fuel cells (PEMFCs), due to their high electrical conductivity, high surface area, as well as superior mechanical and chemical stabilities [1–6]. It has been further reported that there exists an effective interaction between the Pt particles and the CNT support, which can contribute to enhanced electrochemical activity and stability of the Pt particles [7]. Earlier attempts to apply a CNT layer or a blend layer of CNT/CB by means of an ink-process to serve as a Pt support have suggested that the microporous structure of the CNT layer provides increased active Pt area with an optimized mixture of 50 wt.% CNT with 50 wt.% carbon black [3,4]. In addition to the ink-process spreading method, CNTs have also been directly fabricated on carbon papers by various chemical vapor deposition (CVD) techniques to form a catalyst-support layer for metal particles [5,6]. According to Wang et al. [5], multi-wall carbon nanotubes (MWNT) directly fabricated on carbon paper by the CVD process using elec-

trodeposited Co catalysts showed a strong adhesion to the carbon paper substrate and an increased surface area, i.e., as 50 times larger than that of the carbon paper. Another advantage with using the in situ grown MWNT layer as a Pt support lies in that the electronic pathways at the three-phase zone are guaranteed and thus an improvement in Pt utilization is observed, as compared with the conventional ink-process fabrication method. On the other hand, the polarization performance of the Pt/MWNT-based electrode is still lower than that of the conventional ink-process prepared electrode. This is probably due to the large Pt particles formed on the MWNT surface by electrodeposition, which have a size of about 25 nm compared with 2–4 nm from a commercial Pt/C catalyst. In the subsequent work [6], the authors obtained enhanced Pt utilization when the Pt particle size was reduced to 4 nm via in situ chemical reduction of a Pt precursor solution on MWNTs. Due to the inertness of the MWNT surface, however, the dispersion of the Pt particles on MWNTs showed poor uniformity when there was no acid pre-treatment of the MWNT surface. As a result, the Pt particles had a large size distribution range from 2 to 10 nm. The polarization performance of the Pt/MWNT-based electrode remained very low without brushing an additional gas-diffusion layer on the backside of the carbon paper.

Magnetron sputtering is well-known to be one of the most effective and robust deposition techniques for thin film deposition. It has excellent control over film thickness and uniformity, and is therefore an essential tool in the semiconductor and harddisc industries. Recent studies on using magnetron sputtering technique for Pt

\* Corresponding author. Tel.: +65 6516 8933; fax: +65 6776 3604.

E-mail address: [msechcd@nus.edu.sg](mailto:msechcd@nus.edu.sg) (D.H.C. Chua).

deposition have shown that even with a reduced Pt loading, an overall increase in Pt utilization and enhanced Pt–CNT interaction are observed [8–12]. In this study, an integrated Pt/CNT layer is prepared for PEMFC electrodes by in situ growth of a dense CNT layer on carbon paper using a thermal CVD technique followed by direct sputter-deposition of Pt nanodots on to the CNT layer. Enhanced catalytic performance of the Pt/CNT catalyst for cathode reaction is observed in a PEMFC via polarization curve measurements. Morphological and microstructural characterizations of the CNT layer and the sputter-deposited Pt catalysts have been carried out by means of scanning electron microscopy (SEM) and transmission electron microscopy (TEM).

## 2. Experimental

In this work, CNTs were directly grown on Toray™ carbon paper TGPH090 through a thermal chemical vapor deposition (CVD) process, which has a suitable growth temperature and is easy to scale up [13]. Carbon paper sputtered with a thin iron layer was placed into a tube furnace at ambient pressure and then heated to 600 °C in a flow of 100 sccm Ar + 5 vol.% H<sub>2</sub> flow. After holding for 30 min, the temperature was raised to 750 °C and C<sub>2</sub>H<sub>4</sub> was introduced for CNT growth at 20 sccm for 1 h. After growth, C<sub>2</sub>H<sub>4</sub> was cut off and the system was then cooled down to room temperature. Pt catalysts were sputter-deposited on to the CNT-grown carbon paper at room temperature by the same sputtering system for Fe deposition. The loading of 0.04 mg cm<sup>-2</sup> Pt was determined by weight difference of the CNT-grown carbon paper before and after sputter-deposition. The microstructure of the composite CNT layer with sputtered Pt catalyst was characterized by means of SEM and TEM. To prepare the membrane–electrode assembly (MEA) for polarization testing, a conventional ink-process prepared 0.2 mg cm<sup>-2</sup> Pt catalyzed anode and a 0.04 mg cm<sup>-2</sup> Pt-sputtered cathode were hot-pressed with a Nafion™ 112 membrane (140 °C, 20 atm, 90 s). Before hot-pressing, the Pt/CNT-based electrode was brushed with 1 mg PTFE on the backside of the carbon paper to increase the hydrophobicity of the electrode. Polarization curves were measured at 80 °C with a 5 cm<sup>2</sup> fuel cell test station (ElectroChem. Inc.). The H<sub>2</sub> and O<sub>2</sub> gases were fully humidified before feeding into the cell. The stoichiometry of the feed was 2 for the anode and 1 for the cathode with an initial 100 sccm flow, respectively. For comparison, a conventional reference electrode was fabricated by spraying a gas-diffusion layer (GDL) from a VXC72R and PTFE mixture (weight ratio of C to PTFE was 70:30; carbon loading was 1.4 mg cm<sup>-2</sup>), followed by spreading a catalyst layer (CL) that consisted of 0.04 mg cm<sup>-2</sup> Pt/C catalyst (40 wt.% Pt/VXC72R, Johnson–Matthey Corp.) and 0.02 mg cm<sup>-2</sup> Nafion (Dupont). Furthermore, in order to evaluate the effectiveness of the in situ grown CNT layer as support for the Pt catalyst by sputter-deposition, another reference electrode was prepared by sputtering Pt catalyst on a CNT/CB blend layer according to the procedure of Kim et al. [4]. The CNT/CB blend layer was made from a mixture of commercial CNT and carbon black Vulcan XC72R, and it was then spread on to a conventional gas-diffusion electrode prior to Pt sputter-deposition. The commercial CNT used in the present study had an outer diameter of 20–40 nm and a length of 10–50 μm (Shenzhen Nanotech Co. Ltd.), and the weight ratio of CNT to CB was 1:1, which is in accordance with the work of Kim et al. [4].

## 3. Results and discussion

The scanning electron microscope (SEM) images presented in Fig. 1 provide a direct comparison of the top surface of the carbon papers before and after CNT growth. As observed in Fig. 1, a notably high yield of CNTs is obtained after the CVD process. The carbon fibres of the raw carbon paper are fully covered by a wavy CNT

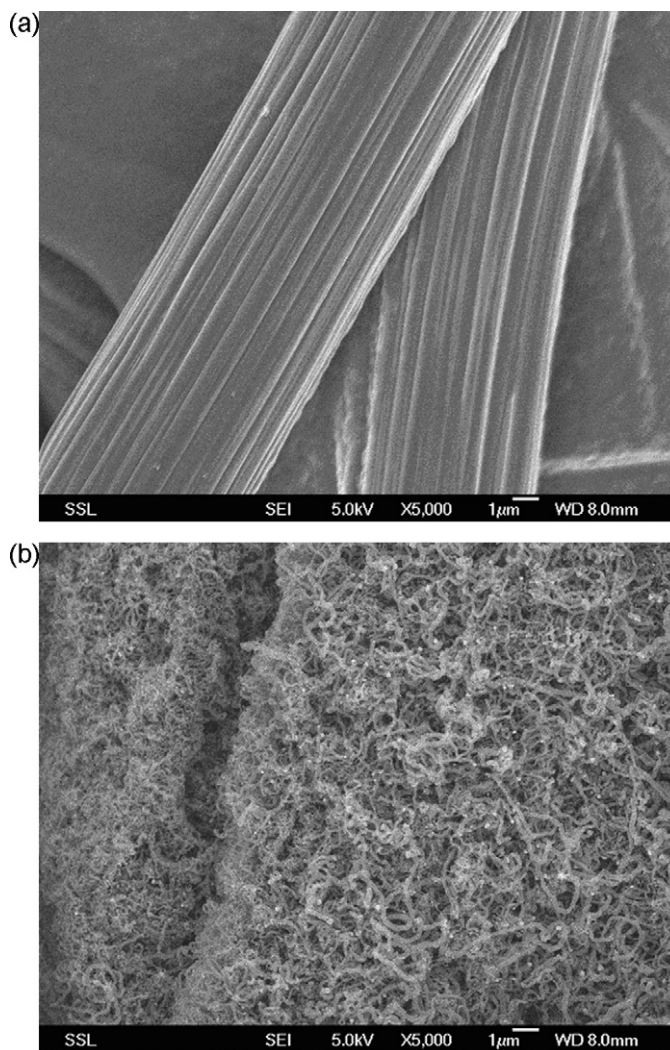
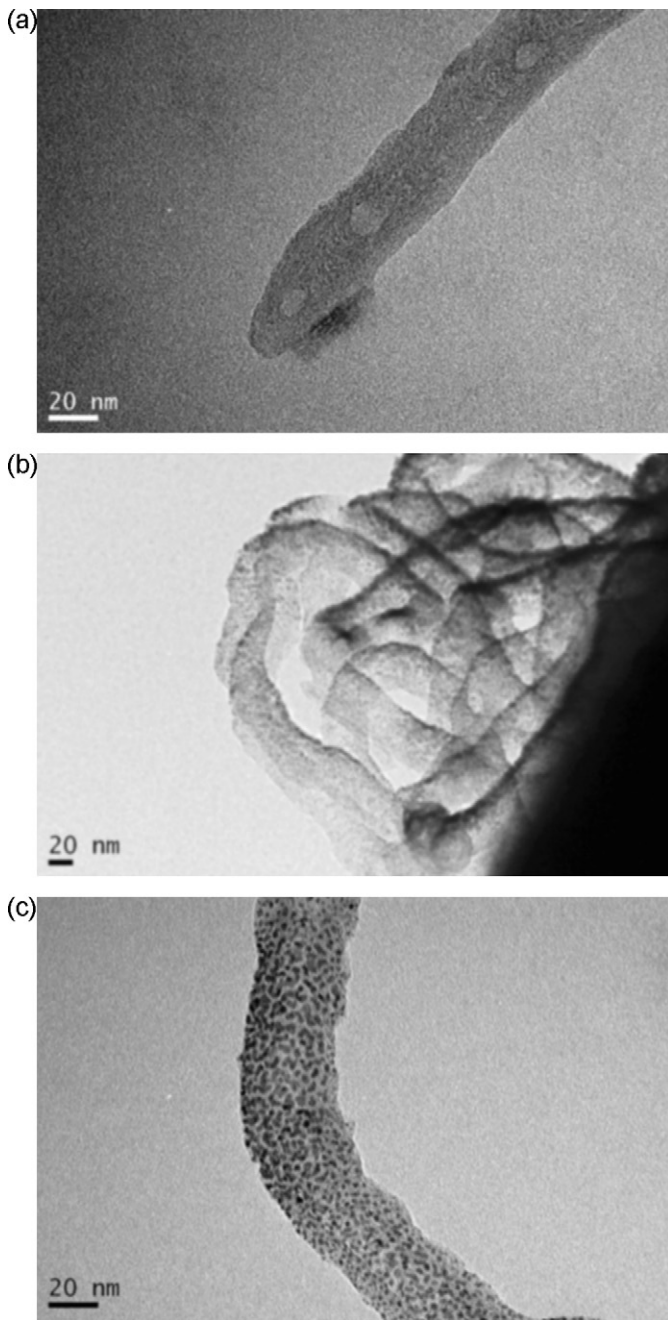


Fig. 1. SEM images of carbon paper surface (a) before and (b) after CNT growth via CVD process.

layer and its gaps and large pores are also filled with CNT clumps to form a continuous surface. The pore size of the CNT layer was observed under 100 nm and the CNT loading was measured to be about 0.25 mg cm<sup>-2</sup>. This results in a dense CNT support layer with a mesoporous structure covering the top of the carbon paper, which tremendously enlarges the porosity and surface area of the pristine carbon paper before growth. A TEM micrograph of the in situ grown CNT peeled off from carbon paper is shown in Fig. 2(a). It can be seen that the CNTs obtained by the thermal CVD process are MWNTs with a typical outer diameter of about 30 nm and an inner diameter of about 10 nm. The Fe catalysts can also be observed as small particles buried inside the tube, which is in accordance with previous studies [14,15]. Unlike metal catalysts deposited by a wet chemical process [5,6], the sputter-deposition of Fe catalysts directly on the carbon paper surface gives the benefit of introducing less metal impurities after CNT growth. Furthermore, it is noteworthy that the as-grown CNTs exhibit very coarse and incontinuous external graphite walls, suggesting that various defects are generated on the CNT skin during growth. This may be greatly in favour of direct Pt deposition, however, due to the presence of a large number of anchoring sites for Pt particles. As previously mentioned, a perfect CNT outer layer has been reported to be strongly hydrophobic with a surface tension higher than 100–200 mN m<sup>-1</sup> [16], hence surface oxidation of CNT is usually necessary for effective deposition of Pt particles on a



**Fig. 2.** TEM images of in situ grown CNT (a) before and (b) after Pt sputter-deposition. (c) Enlarged view of Pt nanodots sputter-deposited on CNT.

CNT support [5,6]. Typically, this requires a series of acid treatment and purification processes thus limiting the overall effectiveness of carbon nanotubes as a catalyst support.

In this study, the in situ grown CNT layer was coated with  $0.04 \text{ mg cm}^{-2}$  Pt catalyst by direct sputter-deposition without any surface modification. Fig. 2(b) and (c) presents the TEM images of the as-deposited Pt nanodots on CNTs. In Fig. 2(b), it can be clearly seen that after Pt sputter-deposition, numerous Pt nanodots are evenly distributed on the outer skin of the CNTs. The Pt loading of  $0.04 \text{ mg cm}^{-2}$  corresponds to a Pt thin film of thickness about 20 nm on a smooth Si substrate. Given the roughness and porosity of the CNT layer substrate, it is understandable that the Pt layer on CNTs is of much lower thickness and thus nanosized Pt particles are deposited and uniformly dispersed on the MWNT surface. According to Fig. 2(c), the grain size distribution of the Pt nanodots on a

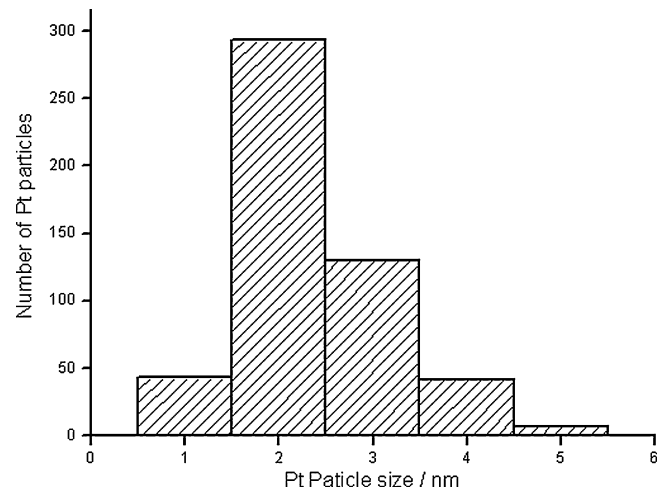


**Fig. 3.** Particle size distribution of Pt on CNT after sputter-deposition based on Fig. 2(c).

single CNT has a relatively small range from 1 to 5 nm. The corresponding size distribution histogram is given in Fig. 3. Most of the sputter-deposited Pt nanodots are less than 4 nm in diameter; the majority have a size distribution of 2–3 nm. It is believed that the mass activity of the Pt catalyst has a strong correlation with the Pt particle size, and the maximum mass activity corresponds to a grain size of approximately 3 nm, as previously reported by Giordano et al. [17]. Moreover, unlike the poor Pt dispersion on a CNT surface without acid treatment according to Wang et al. [6], well-dispersed Pt/CNT catalysts with small particle size are obtained by direct sputter-deposition without any surface oxidation of the CNT support.

The cell performance of MEAs with different GDL and CL combinations on the cathode was investigated by measuring polarization curves (see Fig. 4). As shown in Fig. 4, the Pt-sputtered electrodes exhibit remarkably improved performance compared with the conventional electrode with a carbon black (CB)-based GDL and a commercial Pt/VXC72R catalyst. For the Pt/CNT-based electrode, a high maximum power density of  $595 \text{ mW cm}^{-2}$  is achieved with  $0.04 \text{ mg cm}^{-2}$  Pt on cathode. By contrast, the Pt/VXC72R-based electrode has a maximum power of  $435 \text{ mW cm}^{-2}$  with equal Pt loadings. In addition, the polarization performance of the reference electrode with sputtered Pt on CNT/CB blend layer is also shown in Fig. 4 and gives maximum power density of  $530 \text{ mW cm}^{-2}$ . The

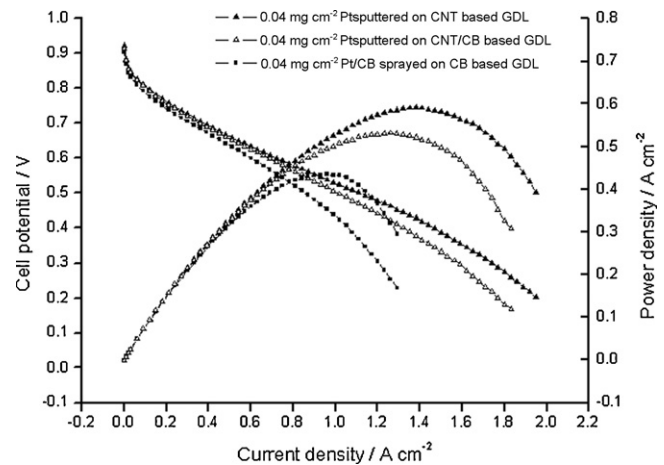


**Fig. 4.** Polarization curves of MEA with Pt/CNT catalyst on cathode, compared with reference MEAs with commercial Pt/VXC72R catalyst and Pt sputtered on CNT/CB blend layer at cathode.

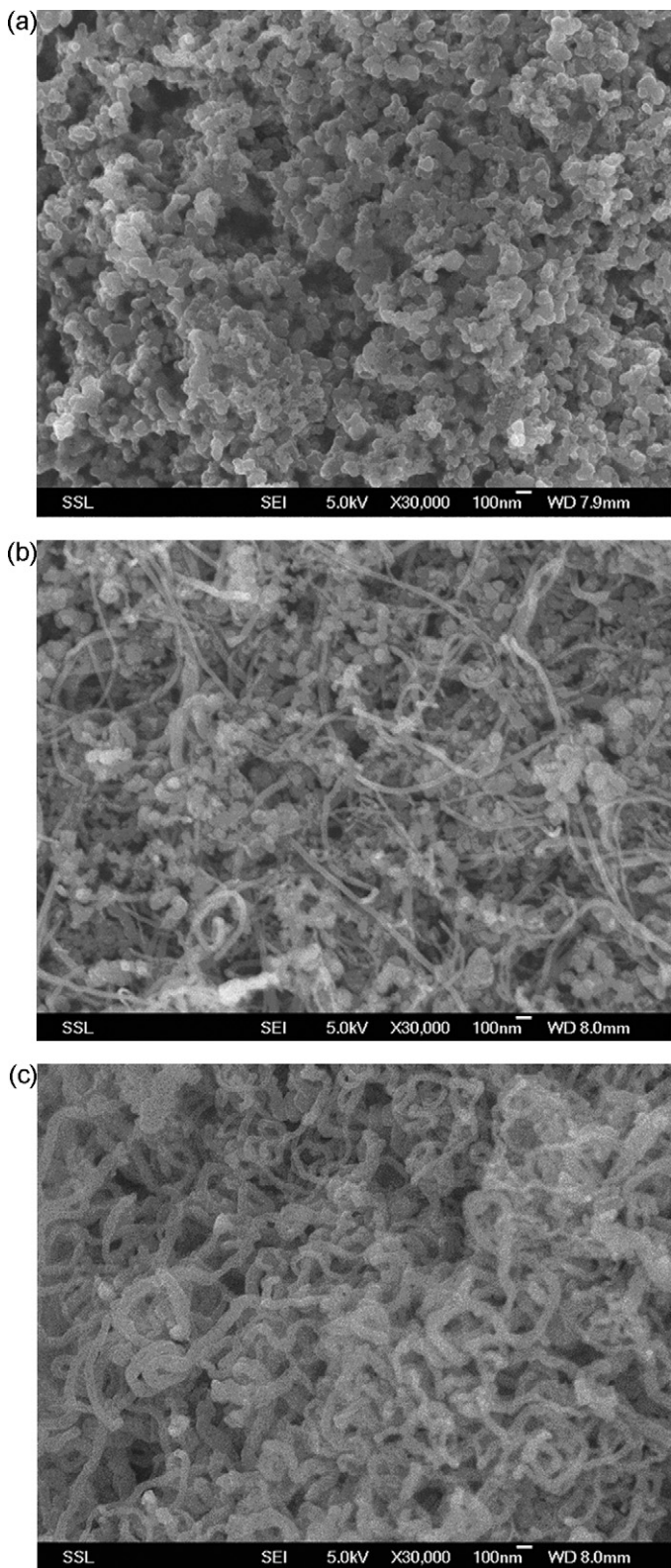


**Fig. 5.** SEM images of top surface of (a) commercial Pt/VXC72R-based catalyst layer, (b) CNT/CB blend layer-based catalyst layer, and (c) in situ grown CNT layer-based catalyst layer.

higher catalytic performance of the sputter-deposited Pt catalysts may arise from the highly localized Pt distribution region at the membrane | electrode interface, which results in a much higher Pt utilization for low Pt loadings [8–10]. Contrary to the sputtered Pt catalyst, the conventional catalyst layer consisting of Pt supported on carbon black has a comparatively large Pt distributed area. It may lead to a covering of the Pt surface by impregnated electrolyte as well as increased mass transport resistance for oxygen and water. Moreover, the polarization results in Fig. 4 suggest that the support layer for the sputter-deposited Pt catalyst may also affect Pt utilization. Hence, further investigation is needed on the different catalyst layers.

A closer observation on the microstructure of the above three electrodes is shown in Fig. 5. The CNT-based electrode shows a distinct structural difference to the conventional carbon black electrode. In a conventional electrode prepared by an ink-process, carbon black VXC72R is the most prevalent GDL and CL material as catalyst support, with particle diameters around 30–50 nm. The carbon powders were made into suspension mixed with binders (typically PTFE in GDL and Nafion in CL) and then sprayed on carbon paper backing. As can be seen in Fig. 5(a), a porous structure with high surface roughness is formed to provide gas and water pathways. However, the porosity of the CB-based electrode is considerably restrained in GDL and CL by the dense carbon black agglomerates. To further increase the electrode surface area, 50 wt.% CNTs were added to a CB-based electrode, as proposed by Kim et al. [4] and Kannan et al. [3]. According to Fig. 5(b), the surface roughness and porosity of the CNT/CB blend layer are greatly enhanced by the porous CNT frame filled with CB particles. As for the CNT layer directly grown on carbon paper, shown in Fig. 5(c), it is evident that a three-dimensional CNT clump is formed with much higher porosity and larger pore size. As a result, the sputtered Pt particles are able to penetrate into the layer thus the overall electrochemical area is increased. It is well known that the catalytic activity of metal/support composite catalysts highly depends on the size and dispersion of the metal nanoparticles as well as their interactions with support materials [7,18]. Therefore, the in situ grown CNT layer combined with a sputter-deposited Pt catalyst exhibits a pronounced improvement in cell performance throughout all polarization regions, in contrast with previous studies where CNT support or sputtering technique is individually used for PEMFC applications. In the activation polarization region, the Pt/CNT catalyst on the cathode gives a higher current density than the reference electrodes, which implies its higher catalytic activity for the oxygen reduction reaction. In addition, a much lower ohmic polarization is observed for the Pt/CNT-based electrode compared with the conventional electrode in the medium current density range. Given that a typical CB-based electrode consists of a gas-diffusion layer and a catalyst layer up to several hundred microns, the CNT-based electrode facilitated with a thin CNT layer as both a GDL and a CL with minimum amount of PTFE would greatly reduce its electrical resistance, as well as the contact resistance between the carbon paper substrate and the CNT layer. For the same reason, the thin integrated CNT GDL and CL would also give much shorter mass transport pathways, resulting in notably improved performance in the high current density region, as shown in Fig. 4. Therefore, the CNT layer grown on carbon paper with a direct sputter-deposited Pt catalyst can provide an effective form of electrode configuration to serve as an integrated GDL and CL for PEMFCs of high efficiency and with low Pt loadings.

#### 4. Conclusions

Dense CNT layers have been directly grown on carbon paper by a CVD process as a Pt support for PEMFC applications. Well-dispersed Pt nanodots sputter-deposited on the CNTs show considerable

improvement in cell performance compared with the conventional Pt catalyst supported on carbon black. The in situ grown CNT layer exhibits extremely high porosity and surface area as a superior support layer for the sputter-deposition of Pt catalyst. Further optimization on the CNT growth and Pt sputtering process is required to obtain Pt/CNT catalysts with controllable particle size and dispersion. In addition, other in situ characterization techniques, including cyclic voltammetry (CV), electrochemical impedance spectroscopy (EIS) and accelerated degradation testing (ADT), are under way to provide a more in-depth understanding of the Pt/CNT on its activity and stability for oxygen reduction.

### Acknowledgements

The authors (TZ and DHCC) acknowledge the partial support from the National University of Singapore R-284-000-028-112/133 and R-284-000-046-123 and NUSNNI for the R.F. Magnetron Sputtering System. TZ acknowledges NUS Research Scholarship funding.

### References

- [1] N. Rajalakshmi, H. Ryub, M.M. Shaijumona, S. Ramaprabha, *J. Power Sources* 140 (2005) 250.
- [2] T. Onoe, S. Iwamoto, M. Inoue, *Catal. Commun.* 8 (2007) 701.
- [3] A.M. Kannan, V.P. Veedu, L. Munukutla, M.N. Ghasemi-Najhad, *Electrochem. Solid-State Lett.* 10 (3) (2007) B47.
- [4] H.T. Kim, J.K. Lee, J. Kim, *J. Power Sources* 180 (2008) 191.
- [5] C. Wang, M. Waje, X. Wang, J.M. Tang, R.C. Haddon, Y.S. Yan, *Nano Lett.* 4 (2) (2004) 345.
- [6] X. Wang, M. Waje, Y.S. Yan, *Electrochem. Solid-State Lett.* 8 (2005) A42.
- [7] S.J. Tauster, S.C. Fung, P.T.K. Baker, J.A. Horsley, *Science* 211 (1981) 1121.
- [8] R. O'Hayre, S.J. Lee, S.W. Cha, F.B. Prinz, *J. Power Sources* 109 (2002) 483.
- [9] N. Toru, S. Masaaki, Y. Kazuaki, *J. Electrochem. Soc.* 12 (2005) 152.
- [10] A. Caillard, C. Charles, R. Boswell, P. Brault, C. Coutanceau, *Appl. Phys. Lett.* 90 (2007) 223119.
- [11] A. Caillard, C. Charles, R. Boswell, P. Brault, *Nanotechnology* 18 (2007) 305603.
- [12] C.L. Sun, L.C. Chen, M.C. Su, L.S. Hong, O. Chyan, C.Y. Hsu, K.H. Chen, T.F. Chang, L. Chang, *Chem. Mater.* 14 (2005) 17.
- [13] W.Z. Li, D.Z. Wang, S.X. Yang, J.G. Wen, Z.F. Ren, *Chem. Phys. Lett.* 335 (2001) 141.
- [14] W.Z. Li, S.S. Xie, L.X. Qian, B.H. Chang, B.S. Zou, W.Y. Zhou, R.A. Zhao, G. Wang, *Science* 274 (1996) 1701.
- [15] Z.W. Pan, S.S. Xie, B.H. Chang, L.F. Sun, W.Y. Zhou, G. Wang, *Chem. Phys. Lett.* 299 (1999) 97.
- [16] E. Dujardin, T.W. Ebbesen, H. Hiura, K. Tanigaki, *Science* 265 (1994) 1850.
- [17] N. Giordano, E. Passalacqua, L. Pino, A.S. Arico, V. Antonucci, M. Vivaldi, K. Kinoshita, *Electrochim. Acta* 36 (1991) 1979.
- [18] A. Gamez, D. Richard, P. Gallezot, F. Gloaguen, R. Faure, R. Durand, *Electrochim. Acta* 41 (1996) 307.